

Diffusion-Weighted MRI Stroke Volume Following Recanalization Treatment is Threshold-Dependent

Rani Gupta Sah^{1,2,3} · Christopher D. d’Este^{1,2,3,4} · Michael D. Hill^{1,2,4} · Moiz Hafeez^{1,2} · Sana Tariq^{2,4} · Nils D. Forkert^{3,4} · Andrew M. Demchuk^{1,2,4} · Mayank Goyal^{1,2,3,4} · Philip A. Barber^{1,2,3,4}

Received: 9 June 2017 / Accepted: 21 September 2017 / Published online: 19 October 2017
© Springer-Verlag GmbH Germany 2017

Abstract

Purpose Infarct lesion segmentation has been problematic as there are a wide range of relative and absolute diffusion-weighted imaging (DWI) and apparent diffusion coefficient (ADC) thresholds that have been used for this purpose. We examined differences of stroke lesion volume and evolution evaluated by magnetic resonance imaging (MRI) during the immediate post-treatment phase (<5 h) and at 24 h.

Methods In this study 33 acute ischemic stroke patients were imaged with MRI <5 h and 24 h post-reperfusion treatment. Lesion volumes were segmented on ADC maps and average DWI using literature cited absolute ADC and relative DWI thresholds. The segmented lesion volumes within both time points were compared and the absolute change in lesion volume (infarct growth) between the two time points was calculated and compared using Bland-Altman analysis.

Results Lesion volumes differed significantly when different relative DWI or absolute ADC thresholds were used ($p < 0.05$), which held true for baseline as well as follow-up lesions. The median absolute changes in lesion volume

from baseline to follow-up for ADC thresholds of $550 \times 10^{-6} \text{mm}^2/\text{s}$, $600 \times 10^{-6} \text{mm}^2/\text{s}$, $630 \times 10^{-6} \text{mm}^2/\text{s}$ and $650 \times 10^{-6} \text{mm}^2/\text{s}$ were 3.5 ml, 4.2 ml, 4.5 ml, and 6.5 ml, respectively ($p < 0.05$). Likewise, the median absolute changes in lesion volume from baseline to follow-up for DWI thresholds, $k = 0.85, 1.28, 1.64, 1.96,$ and 2.7 were 10.1 ml, 7.3 ml, 5.7 ml, 5.4 ml and 4.2 ml, respectively ($p < 0.05$).

Conclusion Absolute lesion volumes and changes in lesion volumes (infarct growth) measured after recanalization treatment were dependent on absolute ADC and relative DWI thresholds, which may have clinical significance. Standardization of techniques for measuring DWI lesion volumes requires immediate attention.

Keywords Ischemic · Diffusion weighted magnetic resonance imaging · Infarction · Reperfusion

Introduction

An improved understanding of infarct evolution following reperfusion therapy may be an opportunity to therapeutically mitigate secondary injury processes associated with blood flow restoration. Measurement of infarct volume by magnetic resonance imaging (MRI) has been used as a secondary endpoint in many randomized control trials [1, 2]; however, segmentation of infarct volumes, both pre-reperfusion and postreperfusion therapy, has been problematic as there is a wide range of relative and absolute diffusion-weighted imaging (DWI) and apparent diffusion coefficient (ADC) thresholds that have been used for this purpose [3–16].

A major reason for the variations in DWI thresholds used to segment the infarct core is related to the proposed definitions of infarct core and the heterogeneity of study

Authors R.G. Sah and C.D. d’Este both contributed equally to this work.

✉ Philip A. Barber
pabarber@ucalgary.ca

- ¹ Calgary Stroke Program, Departments of Clinical Neurosciences, University of Calgary, 3330 Hospital Drive NW, T2N 4N1 Calgary, AB, Canada
- ² Seaman Family Centre, Foothills Medical Centre, Calgary, Canada
- ³ Department of Radiology, University of Calgary, Calgary, Canada
- ⁴ Hotchkiss Brain Institute, University of Calgary, Calgary, Canada

Table 1 Clinical details of all the patients ($n = 33$)

	Total patients
Demographic characteristics:	
<i>Age (years)</i>	
Median	75
Interquartile range	57–82
Female sex, no. (%)	17 (51)
Clinical characteristics:	
<i>Admission NIHSS score</i>	
Median	15
Interquartile range	12–20
<i>Time from onset to baseline MRI (h)</i>	
Median	4.9
Interquartile range	3.6–6.5
<i>Time from onset to follow-up MRI (h)</i>	
Median	26.5
Interquartile range	24.5–32.5
Imaging characteristics:	
<i>Recanalization</i>	
Good reperfusion (TICI > 2a)	16
Poor reperfusion (TICI ≤ 2a)	7
No recanalization (TICI = 0)	6
No recanalization status	4

NIHSS The National Institutes of Health Stroke Scale, TICI Thrombolysis in Cerebral Infarction scale

designs; therefore, standardization of MRI sequences and threshold-based techniques applied for measuring stroke lesion volumes are overdue. Future clinical therapeutic trials and observational acute stroke studies using MR DWI will require standardization of MRI sequences and threshold-based techniques applied for measuring stroke lesion volumes and to permit comparison between studies.

In this work, we examined the stroke lesion volume and its evolution evaluated by MR imaging during the immediate post-treatment phase (<5 h) and at 24 h. Specifically, we determined whether different ADC and DWI thresholds affect the measurement of lesion volume at two time points after reperfusion: <5 h and 24 h. In addition, we quantified the differences in volumetric change between the two imaging time points measured by the prespecified absolute ADC and relative DWI intensity thresholds and quantified the mean differences by estimating the bias and the limits with which differences will lie with 95% confidence. We hypothesize that the change in stroke lesion volumes between two time points will not depend on the absolute ADC and relative DWI thresholds applied, and therefore provides a standardized metric for future stroke trials.

Material and Methods

Patient Details

This was a prospective single-center study including a total of 33 acute ischemic stroke patients. Reperfusion treatment, either tissue plasminogen activator (tPA), mechanical thrombectomy or both, was administered before MR imaging. Written informed consent was obtained from either the patient or the surrogate. The Calgary Health Regional Ethics Board (CHREB) institutional ethical committee approved the study.

Inclusion criteria were: (i) acute ischemic stroke last seen normal within 12 h as per the ESCAPE trial inclusion criteria [17], (ii) occlusion detected by computed tomography angiography (CTA) with hemispheric stroke involving the middle cerebral artery, posterior cerebral artery, or anterior cerebral artery territory, (iii) age ≥18 years and (iv) MR imaging performed immediately following acute treatment <5 h (baseline), and at 24 h (follow-up) after treatment.

MRI Acquisition

All imaging was performed on a 3.0 T clinical MR scanner (Discovery 750; General Electric Healthcare, Waukesha, WI) using a 12-channel receive-only head neck and spine (HNS) coil. Subjects were positioned supine with head first position into the head coil. Diffusion-tensor imaging (DTI) was performed using a spin echo – echo planar imaging (SE-EPI) sequence (repetition time/echo time [TR/TE] = 9000/94.3 ms, field of view [FOV] = 250–350 mm, flip angle = 90°, number of signals averaged [NSA] = 1, EPI factor = 128, acquisition matrix = 144 × 144 and slice thickness = 5 mm without gap) with diffusion sensitizing gradients ($b = 1000 \text{ s/mm}^2$) applied in 15 directions and one non-diffusion-weighted ($b = 0 \text{ s/mm}^2$) volume.

Reperfusion Assessment

Reperfusion status was determined using the thrombolysis in cerebral infarction (TICI) score based on Intra-arterial Therapy (IAT) on digital subtraction angiography (DSA; [18]). Where DSA was not available, the TICI was assessed using the modified arterial occlusion lesion (mAOL) approach from multi-phase CTA (mCTA) data [17].

Image Processing

The DTI data were motion-corrected by aligning all DW volumes to the $b = 0 \text{ s/mm}^2$ volume using the ANTONIA

Table 2 Median (IQR) baseline and follow-up lesion volumes (ml), and the median absolute change in lesion volumes (ml) from baseline to follow-up for specific ADC thresholds

ADC thresholds	$550 \times 10^{-6} \text{ mm}^2/\text{s}$	$600 \times 10^{-6} \text{ mm}^2/\text{s}$	$630 \times 10^{-6} \text{ mm}^2/\text{s}$	$650 \times 10^{-6} \text{ mm}^2/\text{s}$
Baseline absolute lesion volume (ml)	4.0* (0.2, 14.5)	5.3* (0.6, 21.9)	6.3* (0.9, 26.3)	10.1* (1.1, 28.7)
Follow-up absolute lesion volume (ml)	4.7** (1.3, 25.1)	7.6** (2.8, 34.6)	9.7** (4.4, 41.0)	16.9** (6.7, 53.3)
Median absolute change in lesion volume (ml)	3.5 (0.7, 17.5)	4.2 (1.2, 21.2)	4.5 (1.6, 25.4)	6.5 (1.6, 35.4)

*and ** denote absolute volumes were significantly different for all apparent diffusion coefficient (ADC) thresholds (550, 600, 630, and 650) $\times 10^{-6} \text{ mm}^2/\text{s}$ used for lesion segmentation between baseline and follow-up ($P < 0.05$; Wilcoxon test).

Table 3 Median (IQR) baseline and follow-up lesion volumes (ml), and the median absolute change in lesion volume (ml) from baseline to follow-up for specific DWI thresholds

DWI thresholds	$k = 0.85$ (80%)	$k = 1.28$ (90%)	$k = 1.64$ (95%)	$k = 1.96$ (97.5%)	$k = 2.7$ (99.7%)
Baseline absolute lesion volume (ml)	18.9* (8.4, 52.9)	13.1* (5.1, 41.6)	7.7* (2.1, 30.1)	5.6* (1.1, 22.5)	1.8* (0.2, 13.4)
Follow-up absolute lesion volume (ml)	32.6** (11.0, 63.5)	25.35** (7.0, 46.1)	17.7** (4.3, 39.6)	11.6** (3.3, 34.7)	6.7** (1.9, 28.0)
Median absolute change in lesion volume (ml)	10.1 (2.4, 18.5)	7.3 (1.6, 15.1)	5.7 (2.4, 16.4)	5.4 (1.8, 16.4)	4.2 (1.4, 17.3)

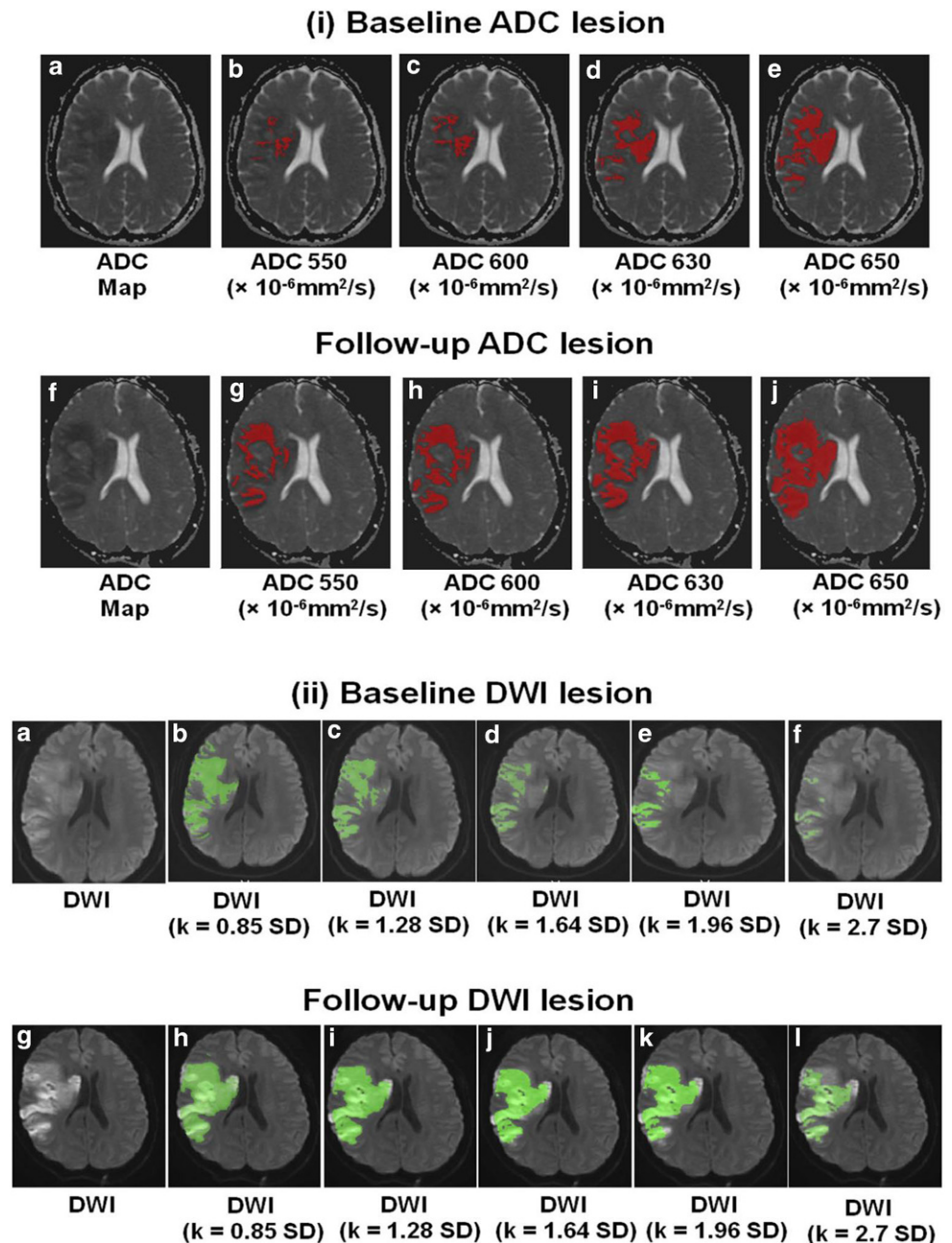
*and ** denote absolute volumes were significantly different at all the diffusion weighted imaging (DWI) intensity thresholds between baseline and follow-up ($P < 0.05$; Wilcoxon test).

software [19]. The pre-processed data were subsequently used to compute an average DWI and the ADC map using the Stejskal-Tanner equation [20]. Lesion volumes were semi-automatically segmented at baseline and follow-up using commonly used ADC thresholds of $550 \times 10^{-6} \text{ mm}^2/\text{s}$, $600 \times 10^{-6} \text{ mm}^2/\text{s}$, $630 \times 10^{-6} \text{ mm}^2/\text{s}$ and $650 \times 10^{-6} \text{ mm}^2/\text{s}$ using the ANTONIA software [7, 9–12, 20]. Lesion segmentation using relative DWI intensity thresholds was performed using MeVisLab software [21]. Therefore, the mean (μ) and standard deviation (σ) of the DWI values in normal contralateral brain tissue was obtained from the average DWI datasets using manually defined regions of interest (ROI) approximately mirroring the visible ischemic region. Different relative thresholds (t) were calculated as $t = (\mu + k \cdot \sigma)$, with $k = 0.85, 1.28, 1.64, 1.96,$ and 2.7 [7, 13–16]. The DWI thresholds were used to segment the lesion using a volume growing approach. The absolute change in lesion volume (infarct growth) between baseline and follow-up was calculated for each ADC and DWI threshold by subtracting the baseline volume from the corresponding follow-up volume. This method for measuring DWI volume is highly correlated to other methodologies, such as voxel-based analysis [22]. Any acquisitions containing hemorrhage were not included in the analysis ($n = 4$ for <5 h, $n = 5$ for 24 h).

Statistical Analysis

Calculation of the distributions of all variables was performed using descriptive statistics, e.g. means, medians, standard deviations, frequency distributions, interquartile range (IQR) and estimated proportions. Non-parametric Wilcoxon test was used for comparisons between baseline and follow-up absolute lesion volumes using different ADC and DWI thresholds. Kruskal-Wallis H (K-independent sample test) was performed for comparisons of the absolute change in lesion volume (infarct growth) from the corresponding ADC and DWI thresholds. We quantified the differences in volumetric change acquired using the pre-specified ADC and DWI thresholds by estimating the bias, which is the mean difference of the volumetric change, and the limits within which most differences will lie at 95% confidence intervals. We estimated these limits from the mean standard deviation of the differences. For example, for the thresholds to agree in terms of these volumetric measurements, we wanted them to be the same for high and low threshold values used for lesion measurement. This can be checked from the Bland-Altman Plot [23]. A p -value of ≤ 0.05 was considered significant. All statistical analyses were performed using Statistical Package for the Social Sciences (SPSS) software (version 19.0; IBM, Armonk, NY).

Fig. 1 Following ischemia reperfusion, the absolute stroke injury volume is dependent on Apparent diffusion coefficient (ADC) and relative Diffusion weighted imaging (DWI) thresholds. In this example, a 45-year-old female (Thrombolysis in Cerebral Infarction [TICI] 2b reperfusion) presenting with a severe stroke at baseline with National Institute of Health Stroke Scale (NIHSS) score of 20 demonstrated M1 occlusion on Computed Tomography Angiogram (CTA). Intravenous-tissue plasminogen activator (tPA) was administered at 3.35 h following stroke symptoms and MR imaging was performed at 4.08 h post-stroke. Reperfusion was confirmed by digital subtraction angiogram (DSA) at this time point. **a–e** The absolute lesion volume determined by applying (i); **f–j** absolute ADC lesion volume at baseline and at follow-up for ADC thresholds of $550 \times 10^{-6} \text{ mm}^2/\text{s}$ to $650 \times 10^{-6} \text{ mm}^2/\text{s}$ and (ii) **a–f**; absolute DWI lesion volume at baseline and **g–i** at follow-up using thresholds of $K = 0.85$ to $k = 2.7$. The ADC and relative DWI thresholds demonstrates considerable variation depending on the threshold used



Results

Subject demographics are summarized in Table 1 and one patient was excluded due to Digital Imaging and Communications in Medicine (DICOM) image corruption. The median absolute lesion volumes for baseline and follow-up were significantly different for each ADC threshold $550 \times 10^{-6} \text{ mm}^2/\text{s}$, $600 \times 10^{-6} \text{ mm}^2/\text{s}$, $630 \times 10^{-6} \text{ mm}^2/\text{s}$ and $650 \times 10^{-6} \text{ mm}^2/\text{s}$ ($p < 0.05$; Table 2). Similarly, the median absolute lesion volumes for baseline and follow-up were significantly different for each DWI threshold $k = 0.85$, 1.28, 1.64, 1.96, and 2.7 ($p < 0.05$; Table 3). Fig. 1 shows the rep-

resentative examples for both diffusion sequences. For both ADC and DWI sequences, there was a significant difference in lesion volume between each time point ($p < 0.05$). Fig. 2 shows the Bland-Altman plots for the absolute change in lesion volumes between baseline and follow-up for the absolute ADC and relative DWI thresholds. Although the bias of agreement was similar when the absolute ADC and relative DWI thresholds were similar, both the bias and limits of agreement increased as the difference of the compared ADC and DWI threshold increases. For example, when comparing lesion growth as determined using the ADC threshold of $550 \times 10^{-6} \text{ mm}^2/\text{s}$ with $600 \times 10^{-6} \text{ mm}^2/\text{s}$, the mean dif-

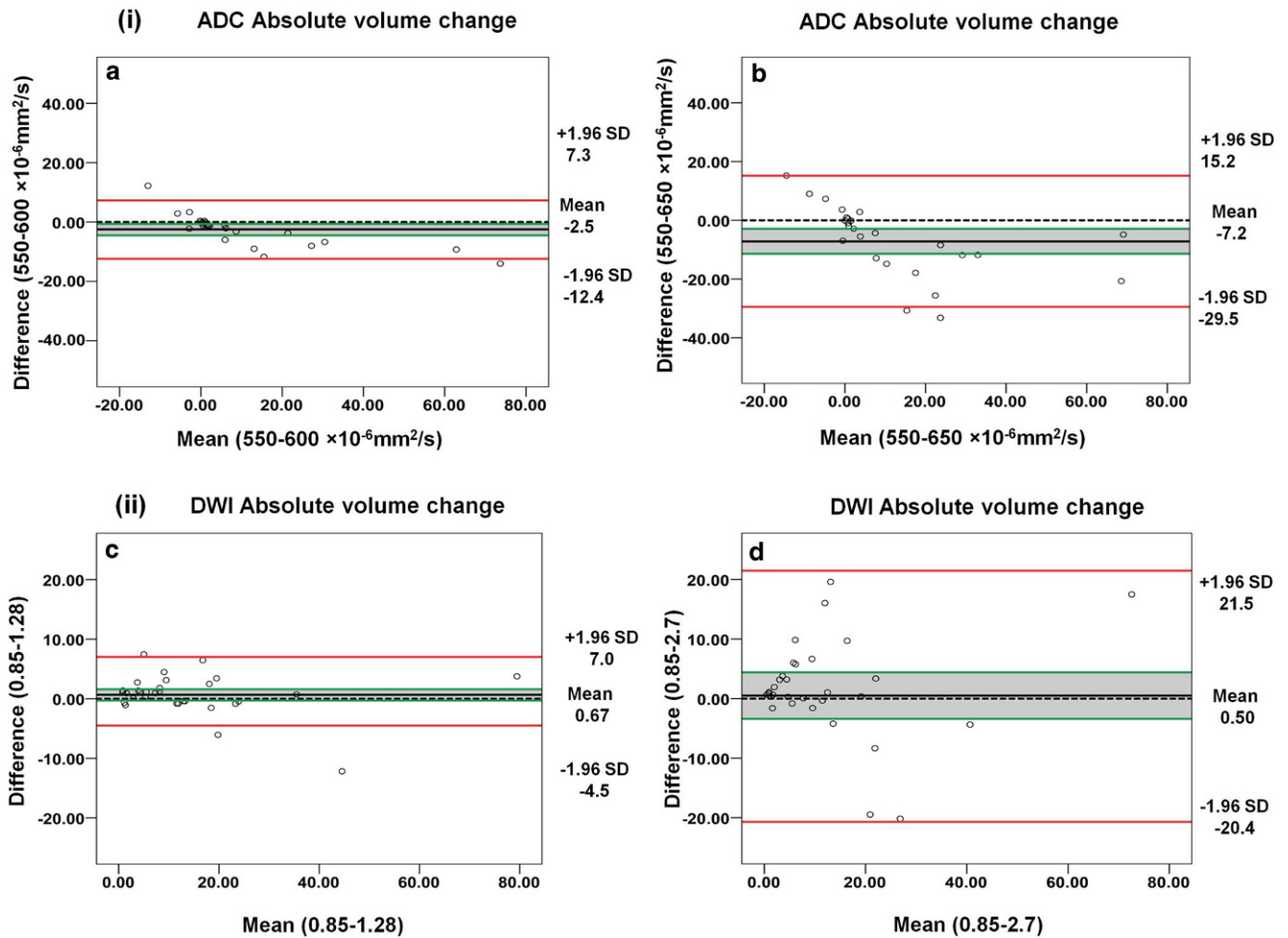


Fig. 2 Shows the Bland-Altman plots comparing (i) apparent diffusion coefficient (ADC) thresholds: **a** absolute change in lesion volume (ml) for 550 and 600 $\times 10^{-6} \text{mm}^2/\text{s}$, **b** absolute change in lesion volume for 550 and 650 $\times 10^{-6} \text{mm}^2/\text{s}$. (ii) Relative diffusion weighted imaging (DWI) thresholds: **c** absolute change in lesion volume (ml) for $k = 0.85$ and $k = 1.28$, **d** absolute change in lesion volume for $k = 0.85$ and $k = 2.7$. In all plots, the Y-axis depicts the difference between the thresholds while the X-axis shows the mean of both threshold values. The bias of agreement is represented by the gap between the X-axis (*bold black line*) and the corresponding zero line (*dashed line*). The *shaded area* represents the confidence intervals around the mean difference. The *red line* represents the $\pm 95\%$ (2 SD) limits of agreement

ference between the measurements is 2.5 ml but the limits of agreement, i. e. 95% CI around the mean difference, can be as high as 12.4 ml. When the difference in thresholds applied increases, for instance, when comparing absolute volume change at thresholds 550 $\times 10^{-6} \text{mm}^2/\text{s}$ and 650 $\times 10^{-6} \text{mm}^2/\text{s}$ the mean difference (the bias agreement) is 7.2 ml and the 95% CI around that mean difference is as high as 29.5 ml. Similar results were obtained for DWI absolute volume change (Fig. 2ii)

Discussion

In this study, the absolute lesion volumes differed when different ADC absolute and DW intensity thresholds were applied at both 5-h and 24-h time points. For instance, the median absolute lesion volume at 24 h for ADC 550 \times

$10^{-6} \text{mm}^2/\text{s}$ versus 650 $\times 10^{-6} \text{mm}^2/\text{s}$ was 16.9 ml versus 4.8 ml, almost a 4-fold difference. Without standardization of the measurement of MR diffusion lesion volumes using absolute ADC thresholds and DWI intensity thresholds, the infarct volumes significantly vary, which will have consequences for interpretation of stroke volume data, comparison of such data between studies, and affect sample size calculations for future clinical trials. Also, contrary to our hypothesis, the absolute lesion volume changes (lesion growth over 24 h after acute revascularization treatment) for both ADC and DWI sequences tended to be threshold dependent, which may have clinical significance. The limits of agreement shown in the Bland-Altman analysis increase as the difference between comparative thresholds increase, and the mean bias of agreement also changes when the threshold comparisons are more disparate. The large difference in volume change between specific thresholds at the

95% CI (limits of agreement) support the conclusion from these data that any two threshold methods are not comparable and that one threshold method cannot reliably replace another threshold method. These observations have significant importance in terms of measuring stroke lesion growth reliably and reproducibly as a suitable outcome measure in MR imaging stroke clinical trials by applying standardized post-imaging analysis methods.

Also of relevance are the limitations of automated thresholding techniques for volumetric analysis of the ischemic lesion. We observed several cases where the ADC and DWI thresholds either failed to segment the lesion completely or underestimated the lesion size compared to visual assessment by experts. Generally, following cerebral ischemia there is restricted diffusivity of water in the extracellular space related to cytotoxic edema, and the diffusivity of water is a time-dependent phenomenon [24]; there is an initial drop in ADC and concomitant increase in DWI [25]. The decline in ADC starts to normalize after 7–10 days, after which the ADC starts to increase supporting the presence of vasogenic edema [25]; however, in some cases, we observed an increase in ADC and a decrease in DWI signal intensity, contradicting the conventional DWI signature of ischemia. This is reflective of the acute increase in water in the extracellular space indicating severe vasogenic edema in the acute phase of ischemia reperfusion [26, 27].

In this study we demonstrated that absolute lesion volumes measured and change in lesion volumes over 24 h after recanalization treatment is dependent on the absolute ADC and relative DWI thresholds used. Standardization of stroke lesion segmentation, either by automated or manual techniques, will be required based on these results. Attempts to salvage ischemic brain tissue with thrombectomy do not always produce a significant clinical benefit in a substantial proportion of stroke patients that receive the therapy. One consideration in the design of future therapeutic stroke trials is the utilization of surrogates of disease progression, such as the temporal change of DWI volume. Measuring an acute change in DWI volume calculated from serially acquired MRI could significantly enrich clinical trial design by reducing sample sizes required to show a biological effect of a potential neuroprotective agent compared with traditional clinical outcome measures or infarct volume measured on MRI at a single time point, e.g. 30-day fluid-attenuated inversion recovery (FLAIR) MRI [28]. We anticipate that our results will support the need for greater standardization of image segmentation methods for measuring acute stroke lesions. This will be imperative to our understanding of reperfusion related secondary lesion growth that will need to be explored in future phase II clinical therapeutic stroke trials, with the aim of improving stroke outcome by attenuating secondary injury processes.

Acknowledgements The authors would like to thank the Heart and Stroke Foundation of Canada for Grant in aid support for the REPERFUSE study, as well as the staff of the Calgary Stroke Program.

Conflict of interests C.D. d'Esterre and P.A. Barber are consultants for Ablynx. R.G. Sah, M.D. Hill, M. Hafeez, S. Tariq, N.D. Forkert, A.M. Demchuk and M. Goyal declare that they have no conflict of interests.

Ethical standards All procedures performed in studies involving human participants were in accordance with the ethical standards of the institutional and/or national research committee and with the 1964 Helsinki declaration and its later amendments or comparable ethical standards. Informed consent was obtained from all individual participants included in the study.

References

- Lansberg MG, Straka M, Kemp S, Mlynash M, Wechsler LR, Jovin TG, Wilder MJ, Lutsep HL, Czartoski TJ, Bernstein RA, Chang CW, Warach S, Fazekas F, Inoue M, Tipirmeni A, Hamilton SA, Zaharchuk G, Marks MP, Bammer R, Albers GW; DEFUSE 2 study investigators. MRI profile and response to endovascular reperfusion after stroke (DEFUSE 2): a prospective cohort study. *Lancet Neurol.* 2012;11:860–7.
- Kidwell CS, Jahan R, Gornbein J, Alger JR, Nenov V, Ajani Z, Feng L, Meyer BC, Olson S, Schwamm LH, Yoo AJ, Marshall RS, Meyers PM, Yavagal DR, Wintermark M, Guzy J, Starkman S, Saver JL; MR RESCUE Investigators. A trial of imaging selection and endovascular treatment for ischemic stroke. *N Engl J Med.* 2013;368:914–23.
- Marks MP, de Crespigny A, Lentz D, Enzmann DR, Albers GW, Moseley ME. Acute and chronic stroke: navigated spin-echo diffusion-weighted MR imaging. *Radiology.* 1996;199:403–8.
- Schlaug G, Siewert B, Benfield A, Edelman RR, Warach S. Time course of the apparent diffusion coefficient (ADC) abnormality in human stroke. *Neurology.* 1997;49:113–9.
- Lansberg MG, Albers GW, Beaulieu C, Marks MP. Comparison of diffusion-weighted MRI and CT in acute stroke. *Neurology.* 2000;54:1557–61.
- An H, Ford AL, Vo K, Powers WJ, Lee JM, Lin W. Signal evolution and infarction risk for apparent diffusion coefficient lesions in acute ischemic stroke are both time- and perfusion-dependent. *Stroke.* 2011;42:1276–81.
- Lansberg MG, Lee J, Christensen S, Straka M, De Silva DA, Mlynash M, Campbell BC, Bammer R, Olivot JM, Desmond P, Davis SM, Donnan GA, Albers GW. RAPID automated patient selection for reperfusion therapy: a pooled analysis of the echoplanar imaging thrombolytic evaluation trial (EPITHET) and the diffusion and perfusion imaging evaluation for understanding stroke evolution (DEFUSE) study. *Stroke.* 2011;42:1608–14.
- Siemonsen S, Löbel U, Sedlacik J, Forkert ND, Mouridsen K, Østergaard L, Thomalla G, Fiehler J. Elevated T₂-values in MRI of stroke patients shortly after symptom onset do not predict irreversible tissue infarction. *Brain.* 2012;135:1981–9.
- Purushotham A, Campbell BC, Straka M, Mlynash M, Olivot JM, Bammer R, Kemp SM, Albers GW, Lansberg MG. Apparent diffusion coefficient threshold for delineation of ischemic core. *Int J Stroke.* 2015;10:348–53.
- Straka M, Albers GW, Bammer R. Real-time diffusion-perfusion mismatch analysis in acute stroke. *J Magn Reson Imaging.* 2010;32:1024–37.
- Na DG, Thijs VN, Albers GW, Moseley ME, Marks MP. Diffusion-weighted MR imaging in acute ischemia: value of apparent diffusion coefficient and signal intensity thresholds in predict-

- ing tissue at risk and final infarct size. *AJNR Am J Neuroradiol.* 2004;25:1331–6.
12. Rosso C, Hevia-Montiel N, Deltour S, Bardin E, Dormont D, Crozier S, Baillet S, Samson Y. Prediction of infarct growth based on apparent diffusion coefficients: penumbral assessment without intravenous contrast material. *Radiology.* 2009;250:184–92.
 13. Neumann-Haefelin T, Wittsack HJ, Fink GR, Wenserski F, Li TQ, Seitz RJ, Siebler M, Mödler U, Freund HJ. Diffusion- and perfusion-weighted MRI: influence of severe carotid artery stenosis on the DWI/PWI mismatch in acute stroke. *Stroke.* 2000;31:1311–7.
 14. Sobesky J, Zaro Weber O, Lehnhardt FG, Hesselmann V, Neveling M, Jacobs A, Heiss WD. Does the mismatch match the penumbra? Magnetic resonance imaging and positron emission tomography in early ischemic stroke. *Stroke.* 2005;36:980–5.
 15. Ma H, Wright P, Allport L, Phan TG, Churilov L, Ly J, Zavala JA, Arakawa S, Campbell B, Davis SM, Donnan GA. Salvage of the PWI/DWI mismatch up to 48 h from stroke onset leads to favorable clinical outcome. *Int J Stroke.* 2015;10:565–70.
 16. Forkert ND, Kaesemann P, Treszl A, Siemonsen S, Cheng B, Handels H, Fiehler J, Thomalla G. Comparison of 10 TTP and tmax estimation techniques for MR perfusion-diffusion mismatch quantification in acute stroke. *AJNR Am J Neuroradiol.* 2013;34:1697–703.
 17. Goyal M, Demchuk AM, Menon BK, Eesa M, Rempel JL, Thornton J, Roy D, Jovin TG, Willinsky RA, Sapkota BL, Dowlatshahi D, Frei DF, Kamal NR, Montaner WJ, Poppe AY, Ryckborst KJ, Silver FL, Shuaib A, Tampieri D, Williams D, Bang OY, Baxter BW, Burns PA, Choe H, Heo JH, Holmstedt CA, Jankowitz B, Kelly M, Linares G, Mandzia JL, Shankar J, Sohn SI, Swartz RH, Barber PA, Coutts SB, Smith EE, Morrish WF, Weill A, Subramaniam S, Mitha AP, Wong JH, Lowerison MW, Sajobi TT, Hill MD; ESCAPE Trial Investigators. Randomized assessment of rapid endovascular treatment of ischemic stroke for the ESCAPE Trial Investigators. *N Engl J Med.* 2015;372:1019–30.
 18. Slater LA, Coutinho JM, Gralla J, Nogueira RG, Bonafé A, Dávalos A, Jahan R, Levy E, Baxter BJ, Saver JL, Pereira VM; STAR and SWIFT investigators. TICI and age: what's the score? *AJNR Am J Neuroradiol.* 2016;37:838–43.
 19. Forkert ND, Cheng B, Kemmling A, Thomalla G, Fiehler J. ANTONIA perfusion and stroke: a software tool for the multi-purpose analysis of MR perfusion-weighted datasets and quantitative ischemic stroke assessment. *Methods Inf Med.* 2014;53:469–81.
 20. Stejskal EO, Tanner JE. Spin diffusion measurements: spin echoes in the presence of a time-dependant field gradient. *J Chem Phys.* 1965;42:288–92.
 21. Ritter F, Boskamp T, Homeyer A, Laue H, Schwier M, Link F, Peitgen HO. Medical image analysis. *IEEE Pulse.* 2011;2(6):60–70. <https://doi.org/10.1109/MPUL.2011.942929>.
 22. Hassen WB, Tisserand M, Turc G, Charron S, Seners P, Edjlali M, Legrand L, Lion S, Calvet D, Naggara O, Mas JL, Meder JF, Baron JC, Oppenheim C. Comparison between voxel-based and subtraction methods for measuring diffusion-weighted imaging lesion growth after thrombolysis. *Int J Stroke.* 2016;11:221–8.
 23. Bland JM, Altman DG. Statistical methods for assessing agreement between two methods of clinical measurement. *Lancet.* 1986;327:307–10.
 24. Hossman KA. Pathophysiological basis of translational stroke research. *Folia Neuropathol.* 2009;47:213–27.
 25. Desai V, Shen Q, Duong TQ. Incorporating ADC temporal profiles to predict ischemic tissue fate in acute stroke. *Brain Res.* 2012;1458:86–92.
 26. Branston NM, Bell BA, Hunstock A, Symon L. Time and flow as factors in the formation of postischemic edema in primate cortex. *Adv Neurol.* 1980;28:291–8.
 27. Crockard A, Iannotti F, Hunstock AT, Smith RD, Harris RJ, Symon L. Cerebral blood flow and edema following carotid occlusion in the gerbil. *Stroke.* 1980;11:494–8.
 28. Ciccone A, Valvassori L, Nichelatti M, Sgoifo A, Ponzio M, Sterzi R, Boccardi E; SYNTHESIS Expansion Investigators. Endovascular treatment for acute Ischemic stroke. *N Engl J Med.* 2013;368:904–13.